

## Platinum Complex as a Nanomolar Protein Kinase Inhibitor

Douglas S. Williams, Patrick J. Carroll, and Eric Meggers\*

Department of Chemistry, University of Pennsylvania, 231 S. 34th Street, Philadelphia, Pennsylvania 19104

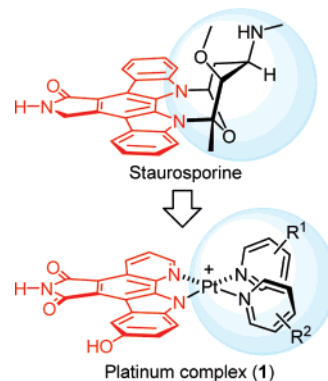
Received October 26, 2006

A pyridocarbazole platinum complex, which matches the overall shape of the natural product staurosporine, binds with high affinity at the adenosine triphosphate binding site of glycogen synthase kinase 3 (GSK-3 $\alpha$ ).

An important objective for the discovery of compounds with new and unique biological activities is the development of methods for the straightforward synthesis of molecular scaffolds with defined three-dimensional shapes.<sup>1</sup> We recently started a research program that explores the scope of using metal complexes to accomplish this goal.<sup>2,3c</sup> In our concept, structures are built from a metal center, with the main function of the metal being to organize the organic ligands in the three-dimensional space. Following this strategy, we disclosed over the last 2 years a series of simple but highly potent ruthenium-based protein kinase inhibitors that mimic the overall shape of the family of indolocarbazole alkaloids (e.g., staurosporine).<sup>2–6</sup>

\* To whom correspondence should be addressed. E-mail: meggers@sas.upenn.edu.

- (1) Biologically relevant chemical space: Koch, M. A.; Schuffenhauer, A.; Scheck, M.; Wetzel, S.; Casaulta, M.; Odermatt, A.; Ertl, P.; Waldmann, H. *Proc. Natl. Acad. Sci. U.S.A.* **2005**, *102*, 17272–17277.
- (2) (a) Bregman, H.; Williams, D. S.; Atilla, G. E.; Carroll, P. J.; Meggers, E. *J. Am. Chem. Soc.* **2004**, *126*, 13594–13595. (b) Williams, D. S.; Atilla, G. E.; Bregman, H.; Arzoumanian, A.; Klein, P. S.; Meggers, E. *Angew. Chem., Int. Ed.* **2005**, *44*, 1984–1987. (c) Bregman, H.; Williams, D. S.; Meggers, E. *Synthesis* **2005**, 1521–1527. (d) Bregman, H.; Carroll, P. J.; Meggers, E. *J. Am. Chem. Soc.* **2006**, *128*, 877–884. (e) Atilla-Gokcumen, G. E.; Williams, D. S.; Bregman, H.; Pagano, N.; Meggers, E. *ChemBioChem* **2006**, *7*, 1443–1450.
- (3) Structures of coordination compounds bound reversibly to proteins through their ligands: (a) Cherrier, M. V.; Martin, L.; Cavazza, C.; Jacquamet, L.; Lemaire, D.; Gaillard, J.; Fontecilla-Camps, J. C. *J. Am. Chem. Soc.* **2005**, *127*, 10075–10082. (b) Contakes, S. M.; Juda, G. A.; Langley, D. B.; Halpern-Manners, N. W.; Duff, A. P.; Dunn, A. R.; Gray, H. B.; Dooley, D. M.; Guss, J. M.; Freeman, H. C. *Proc. Natl. Acad. Sci. U.S.A.* **2005**, *102*, 13451–13456. (c) Debreczeni, J. É.; Bullock, A. N.; Atilla, G. E.; Williams, D. S.; Bregman, H.; Knapp, S.; Meggers, E. *Angew. Chem., Int. Ed.* **2006**, *45*, 1580–1585.
- (4) Inorganic medicinal chemistry: (a) Guo, Z.; Sadler, P. J. *Angew. Chem., Int. Ed.* **1999**, *38*, 1512–1531. (b) Farrell, N., Ed. *Coord. Chem. Rev.* **2002**, *232*, 1–230.
- (5) Bioorganometallic and medicinal organometallic chemistry: Jaouen, G., Ed. *Bioorganometallics*; Wiley-VCH: Weinheim, Germany, 2005.
- (6) For ligand-guided binding of Pt complexes to DNA, see for example: (a) Bowler, B. E.; Hollis, L. S.; Lippard, S. J. *J. Am. Chem. Soc.* **1984**, *106*, 6102–6104. (b) Barry, C. G.; Baruah, H.; Bierbach, U. *J. Am. Chem. Soc.* **2003**, *125*, 9629–9637. (c) Jaramillo, D.; Wheate, N. J.; Ralph, S. F.; Howard, W. A.; Tor, Y.; Aldrich-Wright, J. R. *Inorg. Chem.* **2006**, *45*, 6004–6013.

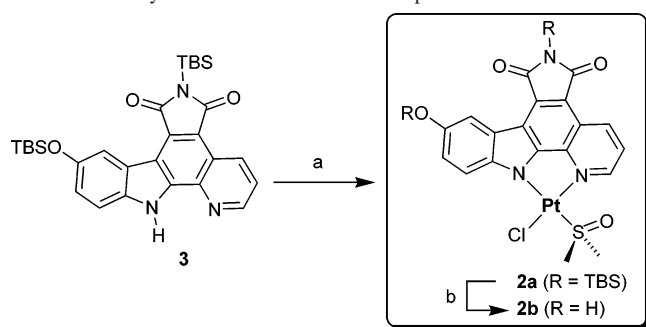


**Figure 1.** Mimicking the overall shape of the indolocarbazole alkaloid staurosporine with a simple platinum complex.

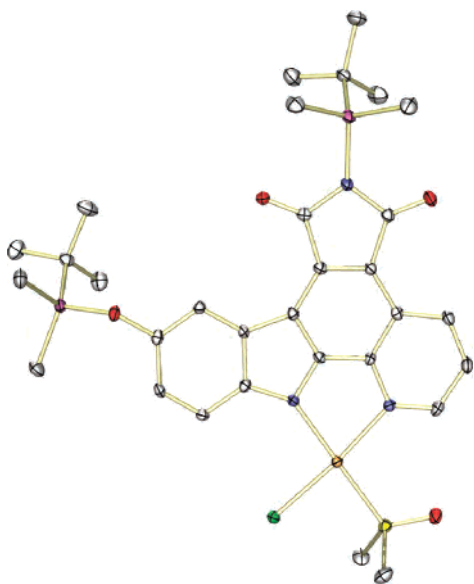
Staurosporine is an adenosine triphosphate (ATP)-competitive protein kinase inhibitor.<sup>7</sup> It adopts a very defined globular structure with the carbohydrate moiety oriented almost perpendicular to the plane of the indolocarbazole heterocycle (Figure 1). The indolocarbazole heterocycle occupies the hydrophobic adenine binding cleft, with the lactam group mimicking the hydrogen-bonding pattern of the adenine base of ATP and the carbohydrate exerting hydrophobic contacts and hydrogen bonds within the globular ribose binding site. Thus, staurosporine matches the shape of the ATP binding site nicely, which makes it a highly potent, albeit unspecific, inhibitor for many protein kinases.

We became interested in evaluating the ability of square-planar platinum complexes to build globular structures. We envisioned matching the overall three-dimensional structure of staurosporine with a simple platinum complex such as **1** in which a chelating pyridocarbazole moiety substitutes the indolocarbazole heterocycle and two pyridines replace the carbohydrate moiety of staurosporine (Figure 1). Because of steric constraints, the two pyridine ligands would have to be oriented more or less perpendicular to the plane of the pyridocarbazole heterocycle and thus define the overall shape of this platinum scaffold **1**. Substituents at the pyridines could then modulate the kinase affinity and selectivity by forming a variety of contacts within the ribose binding site.

- (7) Staurosporine bound to protein kinases: (a) Toledo, L. M.; Lydon, N. B. *Structure* **1997**, *5*, 1551–1556. (b) Lawrie, A. M.; Noble, M. E. M.; Tunnah, P.; Brown, N. R.; Johnson, L. N.; Endicott, J. A. *Nat. Struct. Biol.* **1997**, *4*, 796–801. (c) Prade, L.; Engh, R. A.; Girod, A.; Kinzel, V.; Huber, R.; Bossemeyer, D. *Structure* **1997**, *5*, 1627–1637.

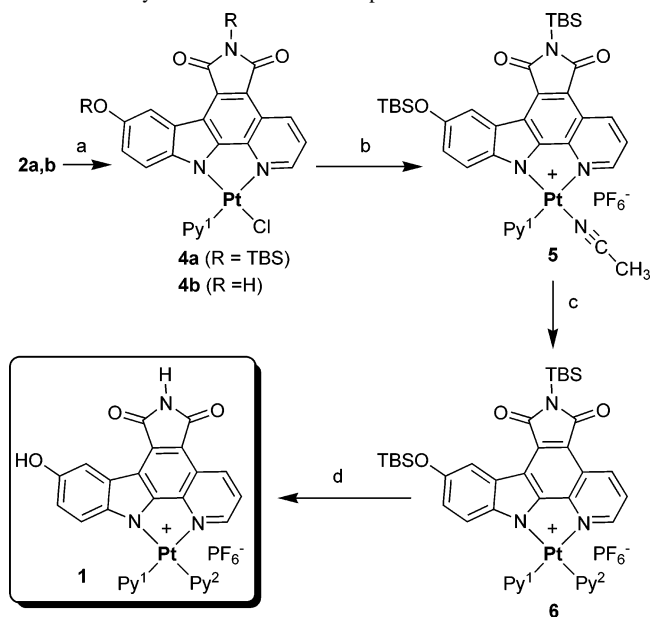
**Scheme 1.** Synthesis of the Precursor Complexes **2a** and **2b**<sup>a</sup>

<sup>a</sup> Reagents and conditions: (a) Pt(DMSO)<sub>2</sub>Cl<sub>2</sub>, K<sub>2</sub>CO<sub>3</sub>, 18:1 toluene/MeOH, 45 °C, 16 h (60% plus 30% of second regioisomer). (b) TBAF, CH<sub>2</sub>Cl<sub>2</sub>. TBS = *tert*-butyldimethylsilyl; TBAF = tetrabutylammonium fluoride.

**Figure 2.** ORTEP drawing of the crystal structure of **2a** with 30% probability thermal ellipsoids.

As a synthetic strategy, we were seeking a cycloplatinated pyridocarbazole intermediate with two substitutionally labile ligands that would serve as a precursor for the economical synthesis of any platinum complex of type **1**. Scheme 1 shows that we obtained such a general precursor, **2a**, by the reaction of the *tert*-butyldimethylsilyl (TBS)-protected pyridocarbazole **3** with Pt(DMSO)<sub>2</sub>Cl<sub>2</sub> (DMSO = dimethyl sulfoxide) in the presence of K<sub>2</sub>CO<sub>3</sub> at 45 °C (60%).<sup>8–10</sup> The other possible regioisomer is formed in lower amounts (30%). A crystal structure of **2a** verifies the regiochemistry, with the DMSO moiety coordinated through the S atom and being arranged trans to the indole (Figure 2). The pyridocarbazole heterocycle is deprotonated at the indole and serves as a bidentate ligand, with the Pt–N coordinative bond distances being 2.05 and 2.08 Å to the indole and pyridine, respectively.

- (8) For the synthesis of Pt(DMSO)<sub>2</sub>Cl<sub>2</sub>, see: Price, J.; Williamson, A.; Schramm, R.; Wayland, B. *Inorg. Chem.* **1972**, *11*, 1280–1284.
- (9) For related platinum complexes with 2-(2'-pyridoindeole), see: (a) Karshedt, D.; Bell, A. T.; Tilley, T. D. *Organometallics* **2004**, *23*, 4169–4171. (b) Karshedt, D.; McBee, J. L.; Bell, A. T.; Tilley, T. D. *Organometallics* **2006**, *25*, 1801–1811.
- (10) For related reactions, see also: (a) Tollari, S.; Cenini, S.; Penoni, A.; Granata, G.; Palmisano, G.; Demartin, F. *J. Organomet. Chem.* **2000**, *608*, 34–41. (b) Cravotto, G.; Demartin, F.; Palmisano, G.; Penoni, A.; Radice, T.; Tollari, S. *J. Organomet. Chem.* **2005**, *690*, 2017–2026.

**Scheme 2.** Synthesis of Platinum Complexes **1** from the Precursor **2a**<sup>a</sup>

<sup>a</sup> Reagents and conditions: (a) Py<sup>1</sup>, CH<sub>2</sub>Cl<sub>2</sub>, reflux 24–48 h (75–83%). (b) AgBF<sub>4</sub>, 2:1 CH<sub>2</sub>Cl<sub>2</sub>/MeCN, reflux, 16 h (81–95%). (c) Py<sup>2</sup>, acetone, reflux, 16 h. (d) TBAF, THF, room temperature, 30 min (35–40% over two steps). TBS = *tert*-butyldimethylsilyl; TBAF = tetrabutylammonium fluoride; Py<sup>1</sup>, Py<sup>2</sup> = pyridine derivatives.

The precursor complex **2a** possesses two leaving groups that can be substituted sequentially. For example, the first substitution is accomplished smoothly by the reaction of **2a** with a pyridine ligand of choice in refluxing CH<sub>2</sub>Cl<sub>2</sub>, providing the platinum complex **4a** in good yields (75–83%). Complex **4a** has the chloride ligand rearranged trans to the indole (Scheme 2). Interestingly, the analogous reaction with the minor regioisomer of **2a** yields an identical product (see the Supporting Information).

A crystal structure of compound **4a** with 4-methoxypyridine as the pyridine ligand (Py<sup>1</sup>) is shown in Figure 3 and verifies the overall coordination geometry. In addition, as expected, the 4-methoxypyridine is oriented almost perpendicularly to the plane of the pyridocarbazole ligand (80.3°).

Next in the synthesis (Scheme 2), removal of the chloride with AgBF<sub>4</sub> and replacement by a labile acetonitrile ligand lead to complex **5** (81–95%), which can then be reacted with the second pyridine ligand under reflux in acetone to yield the bispyridine complex **6**. Finally, deprotection of the TBS groups with tetrabutylammonium fluoride (TBAF) forms complexes of type **1** (35–40% over the last two steps). Alternatively, the TBAF deprotection can be performed at earlier stages of this synthetic scheme.

Following this outlined route, we used a positional scanning protocol (see the Supporting Information) to identify compound **7** (Figure 4) as a nanomolar inhibitor for the kinase GSK-3α. Briefly, the first position was evaluated by TBAF deprotection of **2a** to **2b**, followed by the reaction with 34 different pyridines to give 34 different compounds **4b** (Scheme 2), which were subsequently tested for inhibition of GSK-3α. We identified **4b** with 5-hydroxy-2-methylpyridine (Py<sup>1</sup>) as the most potent compound.

Next, we synthesized the corresponding compound **5**

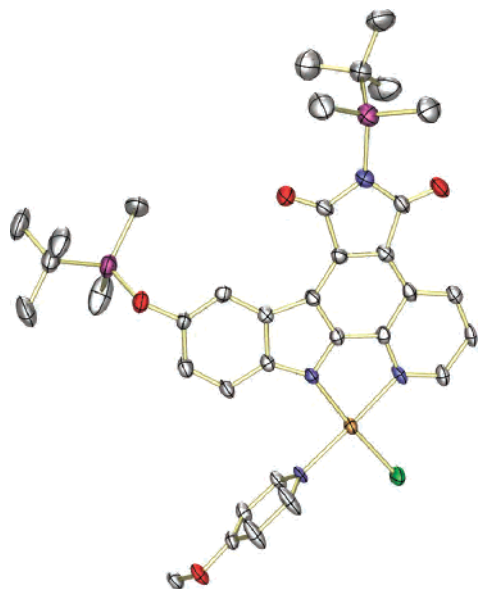


**Figure 3.** Crystal structure of platinum complex **4** with 4-methoxypyridine as the pyridine ligand (Py<sup>1</sup>). ORTEP drawing with 30% probability thermal ellipsoids.

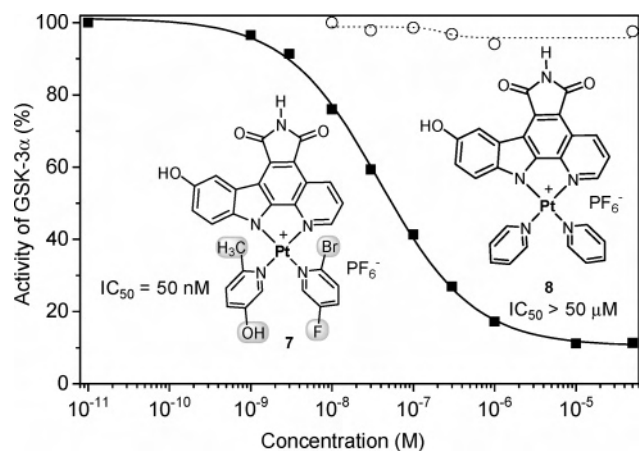


**Figure 4.** IC<sub>50</sub> curves of **7** and **8** against GSK-3 $\alpha$ , obtained by phosphorylation of phosphoglycogen synthase peptide-2 with [ $\gamma$ -<sup>32</sup>P]ATP, followed by precipitation of the phosphorylated substrate on P81 phosphocellulose and measurement of the counts per minutes in a scintillation counter. The ATP concentration was 10  $\mu$ M.

possessing 5-hydroxy-2-methylpyridine as the pyridine ligand Py<sup>1</sup> following Scheme 2, removed the TBS groups, and reacted it with 28 different pyridines to yield a library of 28 complexes **1** (Scheme 2 with steps c and d switched). Again screening against GSK-3 $\alpha$  led to the identification of **7**, having 5-hydroxy-2-methylpyridine cis (Py<sup>1</sup>) and a 2-bromo-5-fluoropyridine ligand trans (Py<sup>2</sup>) to the indole moiety, as the platinum bispyridine compound with the highest affinity for GSK-3 $\alpha$  (Figure 4). The isolated and purified compound **7** exhibits an IC<sub>50</sub> (concentration at which 50% of the enzyme is inhibited) of 50 nM at 10  $\mu$ M ATP.<sup>11,12</sup> With this, **7** has the same affinity for GSK-3 $\alpha$  as staurosporine. For comparison, the plain unsubstituted platinum bispyridine complex **8** (Figure 4) turned out to be not an inhibitor of GSK-3 $\alpha$  at

(11) The platinum complex **7** does not show any signs of decomposition under the assay conditions as established by HPLC (see the Supporting Information).

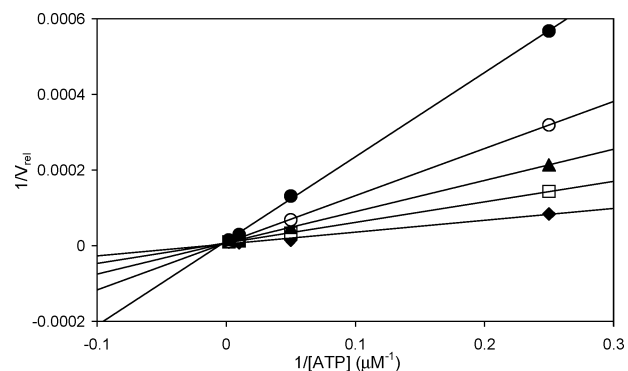


**Figure 5.** Double-reciprocal plots of relative initial velocities ( $V_{rel}$ ) against varying ATP concentrations in the presence of 0 ( $\blacklozenge$ ), 25 ( $\square$ ), 50 ( $\blacktriangle$ ), 100 ( $\circ$ ), and 150 nM ( $\bullet$ ) concentrations of **7**.

all with an IC<sub>50</sub> of larger than 50  $\mu$ M at 10  $\mu$ M ATP.<sup>13</sup> This reflects an increase in the binding affinity by more than a factor of 1000 just by introducing four substituents at the bispyridine periphery.

In order to test if **7** binds as designed to the ATP binding site, we performed a Lineweaver–Burk analysis of relative initial velocities of GSK-3 $\alpha$  at different concentrations of ATP and **7** (Figure 5). The linear plots intersect at  $1/[ATP] = 0$ , demonstrating that **7** binds competitively with respect to ATP. Additionally, methylation of the imide nitrogen of **7** abolishes the activity almost completely (IC<sub>50</sub> > 100  $\mu$ M), consistent with the assumption that the imide hydrogen is involved in hydrogen bonding within the adenine binding cleft.

In conclusion, we here introduced a simple platinum scaffold that binds to the ATP binding site of a protein kinase. As a proof-of-principle, we demonstrated that the derivatization of the periphery of this scaffold can markedly modulate the inhibition properties. Although such platinum complexes will most likely not be suitable for cellular applications because of their charge and lower robustness compared to related ruthenium complexes, we envision that this methodology can serve as a tool for the exploration of chemical space in ATP binding sites of kinases. In this respect, the accessibility of pyridine ligands together with the straightforward synthetic route of platinum complexes should allow for the generation of large libraries of platinum complexes followed by screening against panels of kinases.

**Acknowledgment.** We gratefully acknowledge support from the U.S. National Institutes of Health (1 R01 GM071695-01A1) and the Camille and Henry Dreyfus Foundation. E.M. thanks the Alfred P. Sloan Foundation for a Research Fellowship.

**Supporting Information Available:** Experimental details, spectroscopic data, and crystallographic data. This material is available free of charge via the Internet at <http://pubs.acs.org>.

IC062055T

(12) Complex **7** exists as a mixture of two rotamers as has been verified by NOE experiments (see the Supporting Information).

(13) A more accurate determination of IC<sub>50</sub> was prevented because of limitations in the solubility of **8**.